# Spectroscopic Separation of the Methyl Internal-Rotational Isomers of Thioanisole Isotopomers (C_6H_5S-CH_2D and C_6H_5S-CHD_2)

Jeongmook Lee, So-Yeon Kim, and Sang Kyu Kim*

Department of Chemistry, KAIST, Guseong-dong 373-1, Daejeon 305-701, Republic of Korea

S *Supporting Information*

ABSTRACT: Two distinct rotational isomers of thioanisole-d_1 (C_6H_5S-CH_2D) and thioanisole-d_2 (C_6H_5S-CHD_2) with respect to the internal rotation of the methyl moiety have been identified and characterized spectroscopically using the resonantly enhanced two photon ionization, UV−UV hole burning, and slow-electron velocity map imaging techniques. From the statistical weights, the definite assignment for the specific rotational isomer of each isotopomer has been successfully done, providing isomer-specific ionization energies and vibrational frequencies of S_1/D_0 states. Detailed molecular structures, the methyl internal-rotor barrier, and normal-mode descriptions for selective vibrations are discussed with the aid of density functional theory calculations.
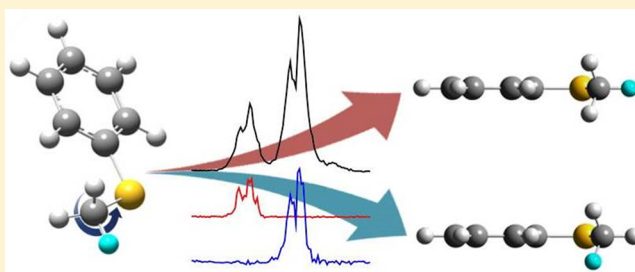
INTRODUCTION

The internal rotation of the methyl (CH_3) moiety with respect to the rest of the molecule has been both extensively and intensively studied for decades as the CH_3 internal rotation with the small barrier influences the intramolecular dynamics in many ways.[1−20] Accordingly, there have been a number of beautiful spectroscopic studies on the CH_3 internal rotor of various molecular systems,[4−18] and the origin of the internal-rotor barrier has been well-documented.[19,20] In the CH_3 internal rotor system, the indistinguishable molecular structure repeats at every 120° rotation, thus giving three identical rotational isomers. When the barrier is small, these rotational isomers interconvert very rapidly via tunneling. On the other hand, if the barrier to internal rotation is large, then one may be able to separate individual rotational isomers, of course, in the case where those are distinguishable. The H/D substitution on the methyl group would be one of the ways for differentiating such rotational isomers with the least changes of the internal rotor dynamics in terms of the barrier height and moment of inertia. The study of the molecular species with partially deuterated methyl groups, in this sense, could be very useful for not only understanding internal-rotor dynamics but also investigating the conformer-specific reaction dynamics.

Herein we have studied rotational isomers of thioanisole-d_1 (C_6H_5S-CH_2D) and thioanisole-d_2 (C_6H_5S-CHD_2). Previous spectroscopic work on thioanisole (C_6H_5S-CH_3) has shown that it adopts the planar geometry in both ground and excited states.[21,22] On the basis of this, two distinct rotational isomers of thioanisole-d_1 or thioanisole-d_2 are clearly identified spectroscopically. Using the UV−UV hole-burning technique, the S_1−S_0 transitions of two rotational isomers have been well separated, giving the detailed vibrational structure of each rotational isomer. The ionization energies and cationic vibrational frequencies of each rotational isomer of thioanisole-d_1 (or thioanisole-d_2) are precisely measured by employing the slow-electron velocity map imaging (SEVI) technique.[23,24] Mode assignments, molecular structures, and energetics are discussed with the aid of density functional theory (DFT) calculations. The subtle changes of nuclear displacement vectors in specific normal modes by partial deuteration of the methyl moiety are carefully examined.

It is noteworthy that this spectroscopic work would be quite useful for the further dynamic study of thioanisole molecules. Recently, photochemistry of thioanisole has been investigated to provide the great opportunity to unravel the conical intersection dynamics. Actually, in the S-CH_3 bond dissociation of the excited thioanisole, it was found that the nonadiabatic transition probability is extremely sensitive to the nature of the vibronic transition of the reactant molecule.[25,26] The topological aspect of the conical intersection and its dynamic role in the photodissociation reaction are main issues in nonadiabatic chemistry.[27−31] In this sense, the dynamic study of thioanisoles with partially deuterated methyl moieties may lead to the better understanding of the conical intersection dynamics, as the subtle changes in normal modes, for instance, could induce big differences in the whole reaction dynamics.
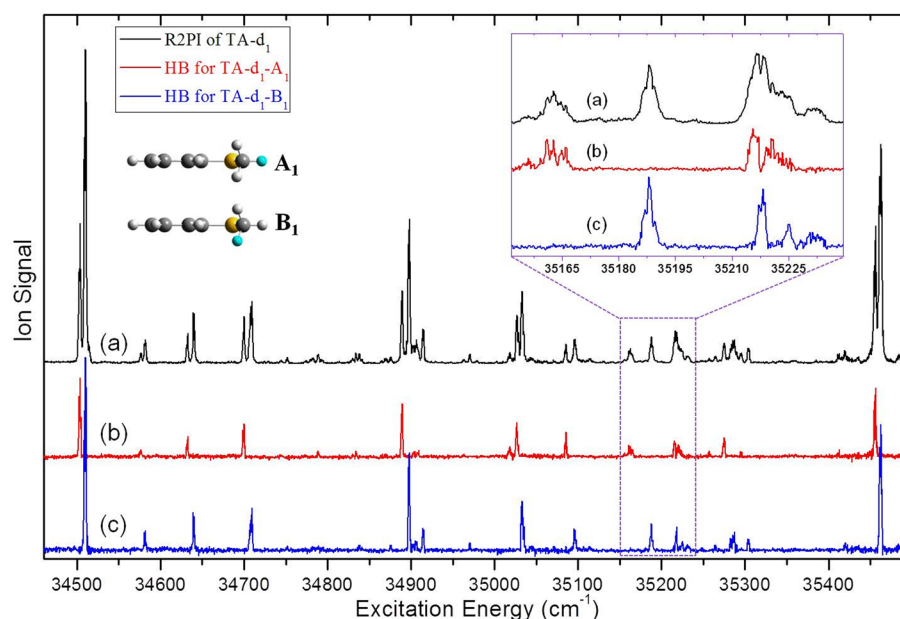
EXPERIMENT

The detailed experimental setup has been previously described.[32] Thioanisole-d_1 and thioanisole-d_2 were purchased (MediGen) and used without further purification. The sample was heated to ∼50 °C, seeded in the argon carrier gas, and

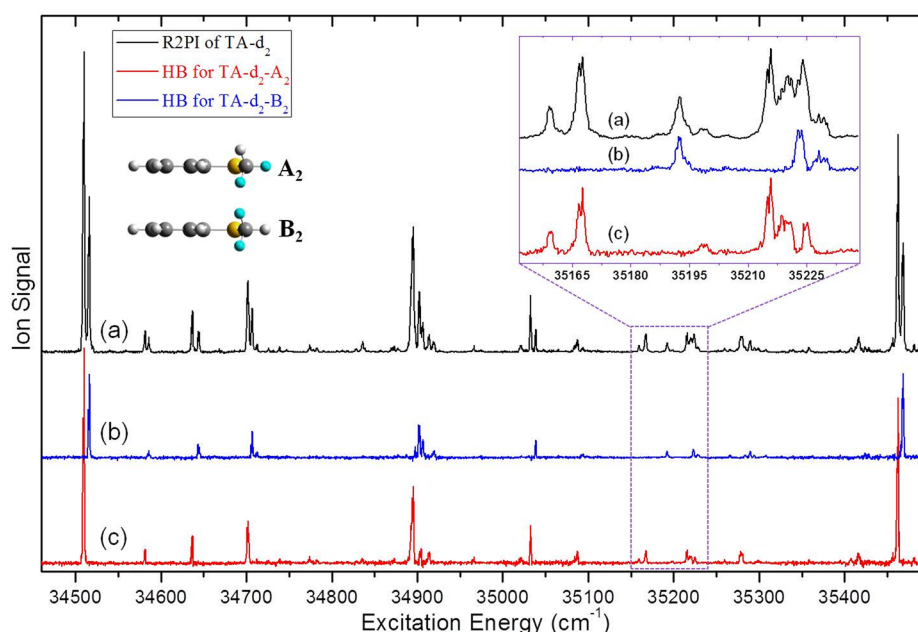**Figure 1.** (a) R2PI spectrum (black) of the mixture of TA-d_1-A$_1$ and TA-d_1-B$_1$. Hole-burning spectra corresponding to the S_1-S_0 excitation spectra of (b) TA-d_1-A$_1$ (red) and (c) TA-d_1-B$_1$ (blue).

Figure 2. (a) R2PI spectrum (black) of the mixture of TA-d_2-A$_2$ and TA-d_2-B$_2$. Hole-burning spectra corresponding to S_1-S_0 excitation spectra of (b) TA-d_2-B$_2$ (blue) and (c) TA-d_2-A$_2$ (red).

expanded into vacuum through a nozzle orifice (General Valve 9, ϕ = 0.5 mm) with a backing pressure of ~3 bar and a repetition rate of 10 Hz. The supersonic jet was skimmed through a 0.5 mm diameter skimmer (Beam Dynamics) before it was intersected by the UV laser pulse at the perpendicular geometry. The pump laser pulse in the 272.5−290.25 nm region was generated by frequency doubling of a dye laser output (Lamda-Physik, Scanmate II) pumped by the second harmonic of a Nd:YAG laser (Spectra-Physics, GCR-150) to be used for obtaining R2PI spectra. For UV−UV hole burning spectroscopy, another dye laser output (Lumonics) pumped by another Nd:YAG (Continuum) was frequency -doubled using a BBO crystal placed on the homemade autotracker to generate

the probe laser pulse. In the hole-burning spectroscopy, the frequency of the pump laser pulse was fixed at one particular transition to depopulate a specific species, whereas the probe laser pulse was scanned to obtain hole-burnt R2PI spectra. For the (1 + 1′) SEVI spectra, the pump laser frequency was fixed at the specific S_1 intermediate state, whereas the ionization laser pulse was used to generate photoelectrons. Photoelectrons were velocity-mapped onto the position-sensitive detector (Burle, ϕ = 40 mm) coupled to a personal-computer-interfaced CCD camera (Sony XC-ST50, 768 × 494 pixels). The SEVI images were processed with the IMACQ acquisition software[33] and reconstructed using a BASEX algorithm.[34] Optimized geometries with relative energies and harmonic vibrational

Table 1. Experimental Values of S_1 Origins and Ionization Potentials of Thioanisoles[a]

thioanisoles (C_5H_6-S-CH_nD_{3-n})	S_1 origin		ionization potential	
	this work	previous work[b]	this work (SEVI)	previous work[b]
TA-h_3	34 504 ± 1	34 506 ± 1	63 899 ± 20	63 906 ± 3
TA-d_1-A_1	34 504 ± 1		63 904 ± 20	
TA-d_1-B_1	34 510 ± 1		63 915 ± 20	
TA-d_2-A_2	34 510 ± 1		63 909 ± 20	
TA-d_2-B_2	34 516 ± 1		63 919 ± 20	
TA-d_3	34 516 ± 1		63 917 ± 20	

[a]All values are given in cm^{-1}. [b]Ref 36.

frequencies for the cationic and ground electronic states of thioanisole-d_1 and thioanisole-d_2 were calculated with the DFT calculations using the B3LYP/6-311++G(3df,3pd) method in the Gaussian 09 package.[35]

■ RESULTS AND DISCUSSION

A. S_1-S_0 Vibronic Bands of Rotational Isomers of Thioanisole-d_1 and $-d_2$. The R2PI spectrum of thioanisole-
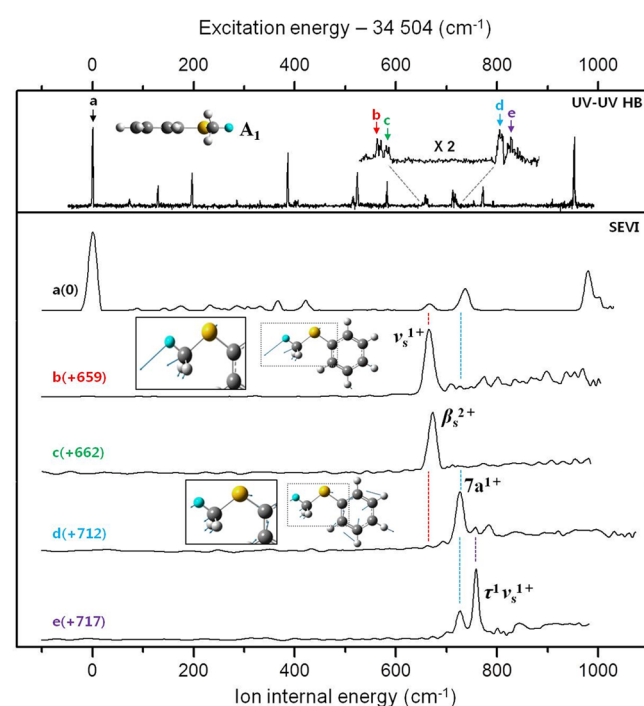
Figure 3. (Upper trace) The hole-burning spectrum corresponding to the S_1-S_0 excitation spectrum of TA-d_1-A_1. (Lower traces) (1 + 1′) SEVI spectra taken via the S_1 origin, 659, 662, 712, and 717 cm^{-1} bands as intermediate states. Nuclear displacement vectors associated with some normal modes of D_0, calculated by DFT (B3LYP/6-311++G(3df,3pd)), are shown.

d_1 shows a series of closely spaced but clearly resolved doublets in the whole spectral region. From the UV−UV hole burning spectroscopy, it is found that the doublet represents vibronic states of two different rotational isomers of thianisole-d_1, Figure 1. Two distinct bands at 34 504 and 34 510 cm^{-1} are then attributed to the S_1-S_0 origins of rotational isomers A_1 and B_1 of thioanisole-d_1, respectively. Here the rotational isomer A_1 represents the conformer where the D atom of the methyl (CH_2D) moiety is on the molecular plane, whereas it is oriented out of the molecular plane for the rotational isomer B_1.

The experimental fact that the intensity of the B_1 origin band is about two times larger than that of the A_1 origin band reflects the statistical weights of two conformers, allowing for the exact identification of each rotational isomer. Namely, there are two different ways for the out-of-plane D atom of the methyl moiety to be oriented in the conformer B_1, whereas there is only one possible orientation in the conformer A_1. It is equivalent to state that in the full 360° internal rotation of the methyl moiety, the statistical probability for the conformer B_1 to be populated is two times higher compared with that for the conformer A_1. The exact 1:2 intensity ratio of the conformer A_1 and B_1 already suggests that the energy difference of two conformers should be very small. In the hole-burnt spectra, the S_1-S_0 vibronic transitions of the conformer A_1 are clearly separated to give its own R2PI spectrum in Figure 1b, and the R2PI spectrum of the conformer B_1 is given in Figure 1c. The spectral pattern of A_1 and B_1 is quite similar in terms of the vibrational frequencies and relative peak intensities, as the normal modes of two species are expected to be not much different. Spectral assignments are appropriately carried out from the SEVI experiment and ab initio calculations. It is noteworthy that the vibrational frequency of the CSC symmetric stretching (ν_s) is somewhat different for two rotational isomers, giving 659 and 678 cm^{-1} for the conformers A_1 and B_1, respectively. This indicates that the nuclear displacement of D or H of the methyl moiety positioned on the molecular plane in the conformer A_1 or B_1, respectively, is heavily involved in the ν_s mode (vide infra).

Similarly, the R2PI spectrum of thioanisole-d_2 also shows a series of closely spaced doublets in the whole spectral region, Figure 2. From the UV−UV hole burning spectroscopy, doublets turn out to be due to two different rotational isomers of thianisole-d_2. Two distinct bands at 34 510 and 34 516 cm^{-1} are thus ascribed to S_1-S_0 origins of rotational isomers A_2 and B_2 of thioanisole-d_2, respectively. Here the rotational isomer A_2 represents the conformer where the H atom of the CHD_2 moiety is out of the molecular plane, whereas one of two D atoms is on the molecular plane. Conversely, in the conformer B_2, the H atom of CHD_2 is on the molecular plane, while both D atoms are positioned out of the molecular plane. The peak intensity of the A_2 origin band is about two times larger than that of the B_2 origin band. This is again quite consistent with the statistical weights of two conformers, allowing for the exact identification of each rotational isomer. This time, there are two different ways for the out-of-plane H atom of the CHD_2 moiety to be oriented in the conformer A_2, whereas there is only one orientation in the conformer B_2. Namely, along the full 360° internal rotation of the methyl moiety, the statistical probability for the conformer A_2 to be populated is two times higher compared with that for the conformer B_2. The S_1-S_0 vibronic transitions of the conformer A_2 and B_2 are clearly separated to

Table 2. Experimental and Calculated Vibrational Frequencies (cm^{-1}) of Thioanisole-d_1[a]

| mode[b] | symmetry | TA-d_1-A$_1$ | | | | TA-d_1-B$_1$ | | | |
| | | S$_0$ | S$_1$ | D$_0$ | | S$_0$ | S$_1$ | D$_0$ | |
		DFT	R2PI	DFT	SEVI	DFT	R2PI	DFT	SEVI
τ	a″	47	**37**	92	**89**	47	**36**	92	**91**
τCH$_2$D	a″	161	**64**	149	**142**	160	**65**	145	**136**
10b	a″	210		172		213		172	
15	a′	190	**196**	185	**188**	190	**199**	190	**189**
β_s	a′	331	**330**	338	**331**	328	**329**	335	**329**
16a	a″	412		383	**367**	412		383	**366**
6a	a′	415	**389**	428	**422**	419	**388**	433	**426**
16b	a″	485		438		485		438	
6b	a′	631	**523**	598	**585**	631	**523**	598	**584**
4	a″	700		644		700		644	
ν_s	a′	671	**659**	663	**666**	694	**678**	678	**679**
7a	a′	718	**712**	733	**727**	718	**708**	727	**718**
11	a″	754		780		754		780	
10a	a″	849		831		850		832	
γ_{as}CH$_2$D	a″	952		908		797		777	
17b	a″	913		965		913		965	
12	a′	996	**953**	980	**980**	996	**953**	980	**980**
β_{as}CH$_2$D	a′	840		838		949		947	
17a	a″	989		1015		989		1015	
1	a′	1045		1022		1045		1023	
5	a″	1003		1029		1003		1029	
18a	a′	1102		1121		1102		1122	
18b	a′	1105		1103		1107		1103	
9b	a′	1183		1192		1183		1192	
9a	a′	1209		1221		1210		1222	
14	a′	1311		1320		1312		1325	
β_sCH$_2$D	a′	1256		1255		1265		1255	
3	a′	1357		1372		1357		1372	
β_sCH$_2$	a′	1465		1429		1449		1441	
19b	a′	1469		1454		1469		1325	
γ_{as}CH$_2$D	a″	1277		1268		1291		1276	
19a	a′	1512		1487		1512		1487	
8b	a′	1607		1546		1607		1546	
8a	a′	1625		1605		1625		1605	
ν_sCD	a′	2280		2292		2263		2277	
ν_{as}CH$_2$	a″	3119		3146		3130		3153	
ν_sCH$_2$	a′	3063		3080		3075		3091	
20a	a′	3165		3191		3165		3191	
7b	a′	3172		3197		3172		3197	
13	a′	3182		3207		3182		3207	
2	a′	3195		3215		3195		3215	
20b	a′	3209		3225		3209		3225	

[a]S$_0$ and D$_0$ frequencies are obtained by using the DFT/6-311++G(3df,3pd) calculation. [b]Normal modes are labeled according to refs 37 and 38. τ is torsion vibration, ν is stretching vibration, β is bending vibration in which vibrating atoms preserve a well-defined plane, and γ is perpendicular bending vibrations with respect to such a plane. In the case of the local vibration of methyl moiety, CH$_n$ is denoted, where n is the number of vibrating hydrogen atoms. The subscript a or as means symmetric or asymmetric character.

give their own R2PI spectra in Figure 2c,b, respectively. The vibrational frequencies and relative peak intensities of A$_2$ and B$_2$ conformers are quite similar, as expected. Similar to the case of thioanisole-d_1, all observed vibronic bands are appropriately assigned from the SEVI and ab initio calculations. The significant vibrational frequency difference is also found only for the CSC symmetric stretching (ν_s) mode, giving 658 and 676 cm^{-1} for the conformer and A$_2$ and B$_2$, respectively. This again confirms that the ν_s mode involves the nuclear displacement of D (or H) of the CHD$_2$ moiety positioned on the molecular plane in the conformer A$_2$ (or B$_2$).

B. Ionization Potentials and Vibrational Structures of Cations from SEVI Spectra. Adiabatic ionization potentials (IPs) of rotational isomers of thianisole-d_1 and thioanisole-d_2 are determined by the SEVI experiments combined with the linear extrapolation method. The (1 + 1′) SEVI spectra are taken as a function of the ionization laser wavelength, while the excitation laser wavelength is fixed at the S$_1$–S$_0$ origin transition energy of each rotational isomer. The kinetic energy of the photoelectron associated with the outmost ring of the SEVI spectrum is plotted with respect to the ionization laser wavelength. The plot is quite linear for all four conformers,

Table 3. Experimental and Calculated Vibrational Frequencies (cm^{-1}) of Thioanisole-d_2[a]

| | | TA-d_2-A$_2$ | | | | TA-d_2-B$_2$ | | | |
| | | S$_0$ | S$_1$ | D$_0$ | | S$_0$ | S$_1$ | D$_0$ | |
mode[b]	symmetry	DFT	R2PI	DFT	SEVI	DFT	R2PI	DFT	SEVI
τ	a″	45	**36**	90	**88**	45	**35**	90	**89**
τCHD$_2$	a″	151	**64**	134	**129**	152	**64**	133	**128**
10b	a″	201		168		200		169	
15	a′	185	**192**	182	**187**	186	**191**	181	**185**
β_s	a′	326	**326**	333	**328**	322		329	**327**
16a	a″	412		383	**372**	412		383	**369**
6a	a′	413	**385**	427	**424**	417	**386**	431	**425**
16b	a″	485		438		485		438	
6b	a′	631	**523**	598	**587**	631	**523**	598	**586**
4	a″	700		644		699		644	
ν_s	a′	668	**658**	659	**665**	691	**676**	676	**682**
7a	a′	715	**706**	726	**720**	716	**707**	728	**723**
11	a″	754		780		754		780	
10a	a″	849		830		850		832	
γ_sCHD$_2$	a″	764		754		734		711	
17b	a″	913		965		913		965	
12	a′	996	**953**	980	**982**	996	**953**	980	**983**
β_{as}CHD$_2$	a′	857		841		846		849	
17a	a″	989		1015		989		1015	
1	a′	1045		1022		1045		1022	
5	a″	1003		1029		1003		1029	
18a	a′	1103		1121		1102		1121	
18b	a′	1106		1104		1107		1103	
9b	a′	1183		1192		1183		1192	
9a	a′	1210		1222		1210		1222	
14	a′	1310		1321		1312		1327	
β_sCHD$_2$	a′	1252		1239		1254		1264	
3	a′	1357		1372		1357		1372	
β_sCD$_2$	a′	1051		1048		1070		1041	
19b	a′	1468		1321		1468		1455	
γ_{as}CHD$_2$	a″	1321		1291		1303		1297	
19a	a′	1512		1487		1512		1487	
8b	a′	1607		1546		1607		1546	
8a	a′	1625		1604		1625		1604	
ν_sCH	a″	3092		3115		3115		3132	
ν_{as}CD$_2$	a″	2320		2338		2315		2334	
ν_sCD$_2$	a″	2225		2234		2214		2225	
20a	a′	3165		3191		3165		3191	
7b	a′	3172		3197		3172		3197	
13	a′	3182		3207		3182		3207	
2	a′	3195		3215		3195		3207	
20b	a′	3209		3225		3209		3225	

[a]S$_0$ and D$_0$ frequencies are obtained by using the DFT/6-311++G(3df,3pd) calculation. [b]Same as in Table 2.

and the simple linear extrapolation to the zero kinetic energy of photoelectron gives the adiabatic IPs of 63 904 and 63 915 cm^{-1} for A$_1$ and B$_1$ conformers of thioanisole-d_1, respectively, whereas IPs of A$_2$ and B$_2$ conformers of thioanisole-d_2 are similarly estimated to be 63 909 and 63 919 cm^{-1}, respectively. These values are uncertain within ±20 cm^{-1}, considering the resolution of the SEVI technique in the current setup. Actually, the same method has been employed for the IP estimation of thioanisole (C$_6$H$_5$SCH$_3$) to give 63 899 cm^{-1}. This value matches well with the previously reported IP value of 63 906 cm^{-1}, which was determined from the zero-electron kinetic energy (ZEKE) spectroscopy.[36] True IP values of four conformers thus may be ~7 cm^{-1} higher than listed in Table 1.

The (1 + 1′) SEVI spectra are acquired using various S$_1$ vibronic states taken as intermediate states. In the SEVI spectra taken via the S$_1$–S$_0$ origins, the D$_0$-S$_1$ origin bands are most strongly observed, while other vibrational bands are only weakly observed for all conformers, Figures 3−6. This indicates that there is no significant structural change upon ionization for all conformers. Overall, most SEVI transitions follow the propensity rule of $\Delta v = 0$. Therefore, the mode assignment of SEVI peaks from the comparison with ab initio values gives the appropriate assignment for the S$_1$ vibronic bands used as intermediate states in obtaining corresponding SEVI spectra. For conformers of A$_1$ and B$_1$, for thioanisole-d_1 (and also for A$_2$ and B$_2$ for thioanisole-d_2), complete series of SEVI spectra were obtained to give the mode assignment for observed S$_1$/D$_0$
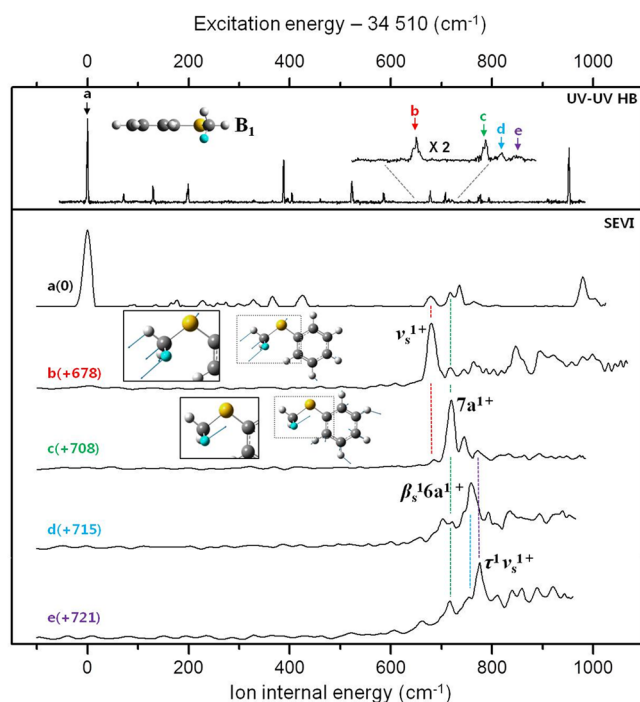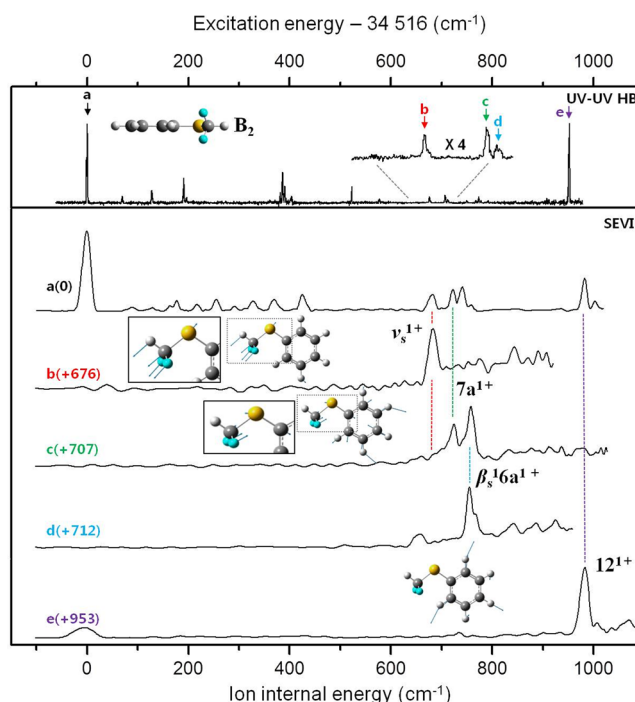
Figure 4. (Upper trace) Hole-burning spectra corresponding to S_1-S_0 excitation spectra of TA-d_1-B_1. (Lower traces) $(1 + 1')$ SEVI spectra taken via the S_1 origin, 678, 708, 715, and 721 cm^{-1} bands as intermediate states. Nuclear displacement vectors associated with the CSC symmetric and CSC asymmetric modes are shown.
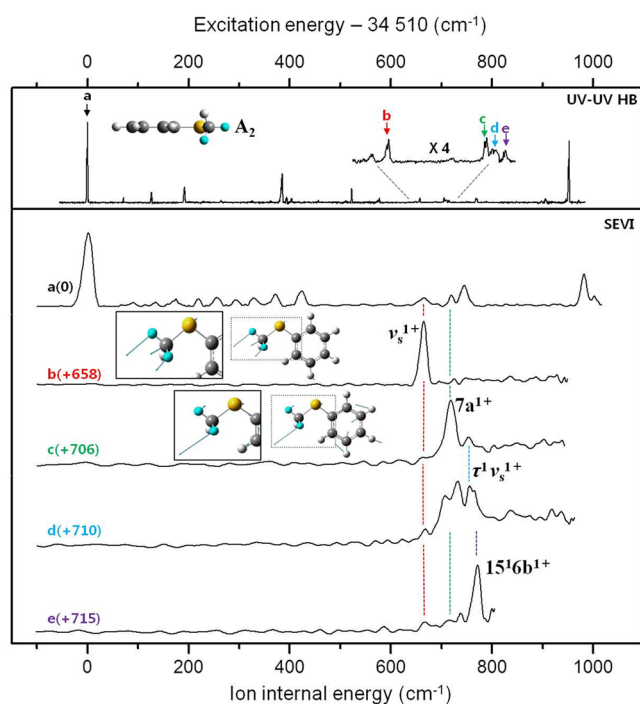
Figure 5. (Upper trace) Hole-burning spectra corresponding to S_1-S_0 excitation spectra of TA-d_2-A_2. (Lower traces) $(1 + 1')$ SEVI spectra taken via the S_1 origin, 658, 706, 710, and 715 cm^{-1} bands as intermediate states. Nuclear displacement vectors associated with some normal modes of D_0, calculated by DFT (B3LYP/6-311+ +G(3df,3pd)), are shown.

vibronic bands, as listed in Tables 2 and 3. (Also see the Supporting Information.) Specifically, in the SEVI spectrum
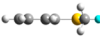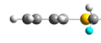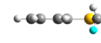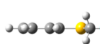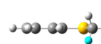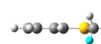

Figure 6. (Upper trace) Hole-burning spectra corresponding to S_1-S_0 excitation spectra of TA-d_2-B_2. (Lower traces) $(1 + 1')$ SEVI spectra taken via the S_1 origin, 676, 707, 712, and 953 cm^{-1} bands as intermediate states. Nuclear displacement vectors associated with the CSC symmetric and CSC asymmetric modes are shown.

taken via the 659 cm^{-1} S_1 band of the conformer A_1 of thioanisole-d_1, the 666 cm^{-1} D_0 band is most strongly observed, as clearly seen in Figure 3. This matches very well with the ab initio value of 663 cm^{-1}, which corresponds to the CSC symmetric stretching mode (ν_s). The 678 cm^{-1} band of the conformer B_1 of thioanisole-d_1 is assigned to ν_s from the SEVI peak observed at 679 cm^{-1}, which agrees well with the calculated value of 678 cm^{-1} (Figure 4). Similarly, the 658 or 676 cm^{-1} R2PI band of the conformer A_2 or B_2 is assigned to ν_s, respectively, from the SEVI band strongly observed at 665 or 682 cm^{-1}, which is in good agreement with the ab initio value of 659 or 676 cm^{-1}, respectively, for the conformer A_2 or B_2 (Figures 5 and 6). Even though the mode assignment according to the propensity rule turns out to be very useful, SEVI spectra taken via some S_1 levels are quite complicated. For example, the SEVI spectrum taken via the 715 or 721 cm^{-1} S_1 band of the B_1 conformer of thioanisole-d_1 shows the broad spectral feature implying the severe mode coupling in the excited state, Figure 4. The mode coupling may originate from the nearby existence of the S_1/S_2 conical intersection, which is not investigated at the present time. This Duschinsky normal-mode mixing seems to be somewhat different for different conformers at several S_1 vibronic states in the spectral region of 550−800 cm^{-1}, implying that the nuclear displacement vectors of these normal modes are extremely sensitive to the isotopic substitution and its conformational orientation.

C. Molecular Structures of Rotational Isomers of Thioanisole-d_1 and -d_2. All conformers of thioanisole-d_1 and -d_2 adopt the minimum energy structure where one C−H(D) bond of the methyl moiety lies on the molecular plane of the benzene moiety, as shown in Figures 1 and 2. This is confirmed by the DFT calculation (B3LYP/6-311++G(3df,3pd)), Table 4. Considering the zero-point energy differences, the conformer

Table 4. Calculated Relative Energies with Zero-Point Correction of Two Rotational Isomers for Thioanisole-d_1 and Thioanisole-d_2 in S_0 and D_0 Using DFT/6-311++G(3df,3pd) [a]

		Thioanisole-d_1		Thioanisole-d_2	
		A_1	B_1	A_2	B_2
S_0	geometry		(more stable)		(more stable)
	ΔE (cm^{-1})	1.10		0.44	
D_0	geometry	(more stable)		(more stable)	
	ΔE (cm^{-1})	9.44		9.22	

[a] A deuterium is depicted as the light-blue sphere.

B_1 is calculated to be ~1.10 cm^{-1} more stable than the conformer A_1 in the ground state, and the conformer A_1 is calculated to be 9.44 cm^{-1} more stable than the conformer B_1 in the cationic ground state. Similarly, the conformer A_2 is predicted to be 9.22 cm^{-1} more stable than the conformer B_2 in the cationic ground state for thioanisole-d_2. This tiny energy difference between two rotational isomers is consistent with the experimental fact that two conformers are populated according to their statistical weights. Also, the experimental IP difference of 11 (or 10) cm^{-1} between A_1 and B_1 (or A_2 and B_2) in Table 1 is very well-reproduced by the calculation previously described. Because the energetics regarding the molecular conformation could largely depend on the calculation method or basis set, the more elaborative theoretical calculations would be desirable in the near future.

The barrier to the methyl internal rotation in the ground electronic state is calculated by the partially relaxed scan of the $C_{(B)}S$-$CH_{(3)}$ dihedral angle, while the geometry of the C_6H_5S moiety is fixed. Here $C_{(B)}$ is the carbon atom of the benzene moiety adjacent to S, whereas $CH_{(3)}$ represents the CH bond of the methyl moiety. The energy is minimum when the $C_{(B)}S$-$CH_{(3)}$ angle is zero and becomes maximum when it is ~60°, giving the internal rotor barrier of 694 cm^{-1}. This somewhat large internal-rotor barrier guarantees the isolation of each rotational isomer stabilized in the deep well, which is consistent with our experimental observation. Because the spectral resolution of this work is not high enough to observe tunneling splitting, we do not have the experimental support for the calculated internal rotor barrier height at the present time. Because the internal rotor barrier is known to be very sensitive to the calculation method and basis set used, however, further theoretical investigations would be desirable for disentangling the detailed structures and energetics involved in the methyl internal rotor of thioanisoles.

CONCLUSIONS

Herein, two distinct rotational isomers of thioanisole-d_1 (C_6H_5S-CH_2D) and thioanisole-d_2 (C_6H_5S-CHD_2) with respect to the methyl internal rotation are clearly identified

spectroscopically. On the basis of the statistical weights, each conformational isomer is unambiguously assigned. Therefore, the IP, S_1 vibronic states, and D_0 cationic vibrational states of each conformer are characterized from the R2PI, UV–UV hole-burning, and SEVI spectroscopic methods. The spectroscopic values are very well explained by the DFT calculations.

ASSOCIATED CONTENT

Ⓢ Supporting Information
Complete author list of ref 35, liquid chromatography and NMR data of samples, full R2PI spectrum of thioanisole-d_1 and thioanisole-d_2, linear relationship between photoelectron kinetic energy and ionization wavelengths, (1 + 1′) SEVI spectra taken via various S_1 intermediate states of thioanisole-d_1 and d_2, and full assignments for all R2PI and SEVI spectra. This material is available free of charge via the Internet at http://pubs.acs.org.

AUTHOR INFORMATION

Corresponding Author
*E-mail: sangkyukim@kaist.ac.kr Tel: (+)82-42-350-2843.

Notes
The authors declare no competing financial interest.

ACKNOWLEDGMENTS

REFERENCES

(1) Kemp, J. D.; Pitzer, K. S. The Entropy of Ethane and the Third Law of Thermodynamics. Hindered Rotation of Methyl Groups. *J. Am. Chem. Soc.* **1937**, *59*, 276–279.

(2) Tamagake, K.; Tsuboi, M.; Hirakawa, A. Y. Internal-Rotational Spectra of Methylamines. II. The Fundamental Torsional Band of CH_2DNH_2. *J. Chem. Phys.* **1969**, *51*, 2592–2603.

(3) Sonoda, Y.; Iwata, S. Theoretical Studies of the Internal Rotation of the Methyl Group in o-, m-, and p-Fluorotoluenes and Their Cations. *Chem. Phys. Lett.* **1995**, *243*, 176–182.

(4) Spangler, L. H.; Pratt, D. W. In *Jet Spectroscopy and Molecular Dynamics*; Hollas, J. M., Phillips, D., Eds.; Chapman &Hall: London, 1995; pp 366−398.

(5) Cvitaš, T.; Hollas, J. M.; Kirby, G. H. Interpretation of Rotational Constants of the First Singlet Excited State of Substituted Benzenes in Terms of Molecular Geometry. *Mol. Phys.* **1970**, *19*, 305−316.

(6) Serrallach, A.; Meyer, R.; Günthard, Hs.H. Methanol and Deuterated Species: Infrared Data, Valence Force Field, Rotamers, and Conformation. *J. Mol. Spectrosc.* **1974**, *52*, 94−129.

(7) McKean, D. C.; Watt, R. A. Vibrational Spectra of Nitromethanes of Internal Rotation and the Effects. *J. Mol. Spectrosc.* **1976**, *61*, 184−202.

(8) Okuyama, K.; Mikami, N.; Ito, M. Internal Rotation of the Methyl Group in the Electronically Excited State: o-, m-, and p-Fluorotoluene. *J. Phys. Chem.* **1985**, *89*, 5617−5625.

(9) Breen, P. J.; Bernstein, E. R.; Seeman, J. I. Supersonic Molecular Jet Spectroscopy of Ethylbenzene, the Ethyltoluenes, and the Diethylbenzenes. *J. Chem. Phys.* **1987**, *87*, 3269−3275.

(10) Tan, X. Q.; Majewski, W. A.; Plusquellic, D. F.; Pratt, D. W. Methyl Group Torsional Dynamics from Rotationally Resolved Electronic Spectra. 1-and 2-Methylnaphthalene. *J. Chem. Phys.* **1991**, *94*, 7721−7733.

(11) Zhao, Z.-Q.; Parmenter, C. S.; Moss, D. B.; Bradley, A. J.; Knight, A. E. W.; Owens, K. G. p-Fluorotoluene. I. Methyl (CH_3 and CD_3) Internal Rotation in the S_1 and S_0 States. *J. Chem. Phys.* **1992**, *96*, 6362−6377.

(12) Yan, S.; Spangler, L. H. Remote Substituent Effects on Methyl Torsional Barriers: trans-p-Amino-p′-methylstilbene. *J. Phys. Chem.* **1995**, *99*, 3047−3052.

(13) Walker, R. A.; Richard, E.; Lu, K. T.; Sibert, E. L., III; Weisshaar, J. C. Intensities of Forbidden Pure Torsional Bands in S_1−S_0 Spectra of Toluenes. *J. Chem. Phys.* **1995**, *102*, 8718−8724.

(14) Ikoma, H.; Takazawa, K.; Emura, Y.; Ikeda, S.; Abe, H.; Hayashi, H.; Fujii, M. Internal Rotation of Methyl Group in o- and m-Toluidine Cations as Studied by Pulsed Field Ionization-Zero Kinetic Energy Spectroscopy. *J. Chem. Phys.* **1996**, *105*, 10201−10209.

(15) Spangler, L. H. Structural Information from Methyl Internal Rotation Spectroscopy. *Annu. Rev. Phys. Chem.* **1997**, *48*, 481−510.

(16) Suzuki, K.; Ishiuchi, S.; Fujii, M. Pulsed Field Ionization-ZEKE Spectroscopy of Cresoles and Their Aqueous Complexes: Internal Rotation of Methyl Group and Intermolecular Vibrations. *Faraday Discuss.* **2000**, *115*, 229−243.

(17) Reid, K. L. Picosecond Time-Resolved Photoelectron Spectroscopy as a Means of Gaining Insight into Mechanisms of Intramolecular Vibrational Energy Redistribution in Excited States. *Int. Rev. Phys. Chem.* **2008**, *27*, 607−628.

(18) Alvarez-Valtierra, L.; Yi, J. T.; Pratt, D. W. Rotationally Resolved Electronic Spectra of 2- and 3-Methylanisole in the Gas Phase: A Study of Methyl Group Internal Rotation. *J. Phys. Chem. B* **2006**, *110*, 19914−19922.

(19) Bickelhaupt, F. M.; Baerends, E. J. The Case for Steric Repulsion Causing the Staggered Conformation of Ethane. *Angew. Chem., Int. Ed.* **2003**, *42*, 4183−4188.

(20) Mo, Y.; Wu, W.; Song, L.; Lin, M.; Zhang, Q.; Gao, J. The Magnitude of Hyperconjugation in Ethane: A Perspective from Ab Initio Valence Bond Theory. *Angew. Chem., Int. Ed.* **2004**, *43*, 1986−1990.

(21) Hoshino-Nagasaka, M.; Isozaki, T.; Suzuki, T.; Ichimura, T.; Kawauchi, S. Molecular Structure of Jet-Cooled Thioanisole Studied by Laser-Induced Fluorescence Spectroscopy and ab initio Calculations: Planar and/or Perpendicular Conformation? *Chem. Phys. Lett.* **2008**, *457*, 58−61.

(22) Hoshino-Nagasaka, M.; Suzuki, T.; Ichimura, T.; Kasahara, S.; Baba, M.; Kawauchi, S. Rotationally Resolved High-Resolution Spectrum of the S-1-S-0 Transition of Jet-cooled Thioanisole. *Phys. Chem. Chem. Phys.* **2010**, *12*, 13243−13427.

(23) Offerhaus, H. L.; Nicole, C.; Lépine, F.; Bordas, C.; Rosca-Pruna, F.; Vrakking, M. J. J. A Magnifying Lens for Velocity Map Imaging of Electrons and Ions. *Rev. Sci. Instrum.* **2001**, *72*, 3245−3248.

(24) Neumark, D. M. Slow Electron Velocity-Map Imaging of Negative Ions: Applications to Spectroscopy and Dynamics. *J. Phys. Chem. A* **2008**, *112*, 13287−13301.

(25) Lim, J. S.; Kim, S. K. Experimental Probing of Conical Intersection Dynamics in the Photodissociation of Thioanisole. *Nat. Chem.* **2010**, *2*, 627−632.

(26) Roberts, G. M.; Hadden, D. J.; Bergendahl, L. T.; Wenge, A. M.; Harris, S. J.; Karsili, T. N. V.; Ashfold, M. N. R.; Paterson, M. J.; Stavros, V. G. Exploring Quantum Phenomena and Vibrational Control in σ* Mediated Photochemistry. *Chem. Sci.* **2013**, *4*, 993−1001.

(27) Yarkony, D. R. Diabolical Conical Intersections. *Rev. Mod. Phys.* **1996**, *68*, 985−1013.

(28) Domcke, W.; Yarkony, D. R.; Koppel, H. *Conical Intersections: Theory, Computation and Experiment*; World Scientific Publishing: Singapore, 2011.

(29) Sobolewski, A. L.; Domcke, W.; Dedonder-Lardeux, C.; Jouvet, C. Excited-State Hydrogen Detachment and Hydrogen Transfer Driven by Repulsive $^1\pi\sigma^*$ States: A New Paradigm for Nonradiative Decay in Aromatic Biomolecules. *Phys. Chem. Chem. Phys.* **2002**, *4*, 1093−1100.

(30) Ashfold, M. N. R.; King, G. A.; Murdock, D.; Nix, M. G. D.; Oliver, T. A. A.; Sage, A. G. πσ* Excited States in Molecular Photochemistry. *Phys. Chem. Chem. Phys.* **2010**, *12*, 1218−1238.

(31) Crespo-Hernandez, C. E.; Cohen, B.; Hare, P. M.; Kohler, B. Ultrafast Excited-State Dynamics in Nucleic Acids. *Chem. Rev.* **2004**, *104*, 1977−2019.

(32) Ahn, D.-S.; Lee, J.; Park, Y. C.; Lee, Y. S.; Kim, S. K. Nuclear Motion Captured by the Slow Electron Velocity Imaging Technique in the Tunnelling Predissociation of the S1Methylamine. *J. Chem. Phys.* **2012**, *136*, 024306.

(33) Li, W.; Chambreau, S. D.; Lahankar, S. A.; Suits, A. G. Megapixel Ion Imaging with Standard Video. *Rev. Sci. Instrum.* **2005**, *76*, 063106.

(34) Dribinski, V.; Ossadtchi, A.; Mandelshtam, V. A.; Reisler, H. Reconstruction of Abel-Transformable Images: The Gaussian Basis-Set Expansion Abel Transform Method. *Rev. Sci. Instrum.* **2002**, *73*, 2634−2642.

(35) Frisch, M. J.; Trucks, G. W.; Schlegel, H. B.; Scuseria, G. E.; Robb, M. A.; Cheeseman, J. R.; Scalmani, G.; Barone, V.; Mennucci, B.; Petersson, G. A. et al. *Gaussian 09*, revision A.1; Gaussian, Inc.: Wallingford, CT, 2009.

(36) Vondrák, T.; Sato, S.; Špirko, V.; Kimura, K. Zero Kinetic Energy (ZEKE) Photoelectron Spectroscopic Study of Thioanisole and Its van der Waals Complexes with Argon. *J. Phys. Chem. A* **1997**, *101*, 8631−8638.

(37) Wilson, E. B., Jr. The Normal Modes and Frequencies of Vibration of the Regular Plane Hexagon Model of the Benzene Molecule. *Phys. Rev.* **1934**, *45*, 706−714.

(38) Varsányi, G.; Kovner, M. A.; Láng, L. *Assignments for Vibrational Spectra of 700 Benzene Derivatives*; Akademiai Kiadó: Budapest, 1973.